Figure S1

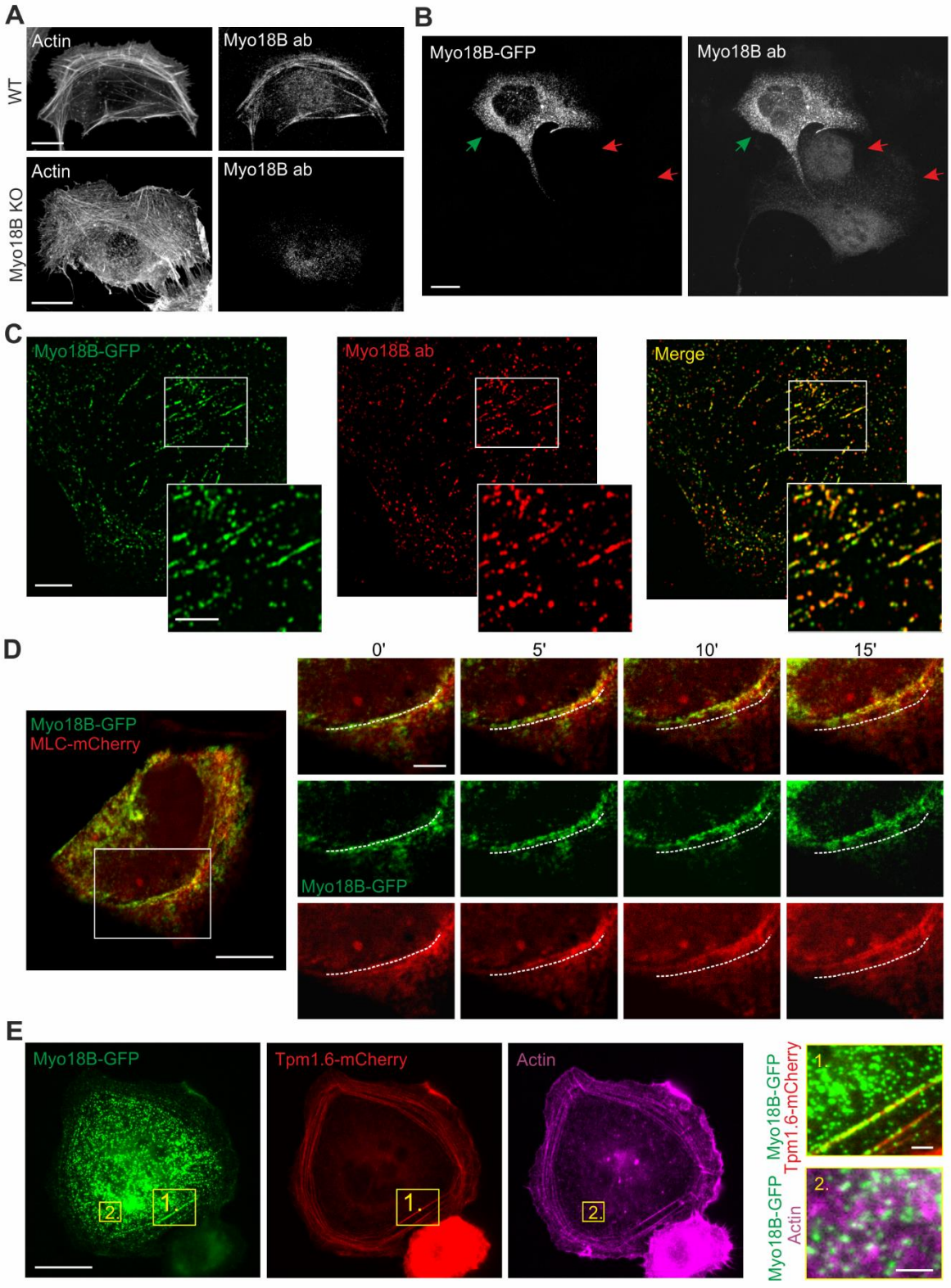
A
Actin
Myo18B ab
WT
Actin
Myo18B ab
Myo18B KO
B
Myo18B-GFP
Myo18B ab
C
Myo18B-GFP
Myo18B ab
Merge
D
0'
5'
10'
15'
Myo18B-GFP
MLC-mCherry
Myo18B-GFP
E
Myo18B-GFP
Tpm1.6-mCherry
Actin
1.
2.
Myo18B-GFP
Tpm1.6-mCherry
Myo18B-GFP
Actin

Figure S1 Myosin-18B localization in U2OS cells. Related to Figure 1. (**A**) Representative images of wild-type (WT) and myosin-18B knockout (Myo18 KO) cells where endogenous myosin-18B and F-actin were visualized by an antibody from LSBio (cat # LS-C403352) and phalloidin, respectively. Bars, 10 µm. (**B**) The myosin-18B antibody from LSBio recognizes exogenously expressed myosin-18B-GFP in myosin-18B knockout cells. The myosin-18B-GFP expressing cell is indicated with a green arrow and the two non-transfected knockout cells with red arrowheads. Bars, 20 µm. (**C**) Representative SIM images of wild-type U2OS cells expressing myosin-18B-GFP. Please note that the myosin-18B antibody from LSBio stains majority of myosin-18B-GFP puncta in these cells. Bars, 5 µm and 2 µm in the main images and magnified panels, respectively. (**D**) Time-lapse imaging of GFP tagged myosin-18B and mCherry tagged myosin light chain (MLC) in U2OS cells. The dashed line in the insets indicates the position of a MLC and myosin-18B –rich stress fiber in the beginning of the time-lapse movie. Please note that the myosin-18B-GFP puncta undergo retrograde flow with the MLC-rich stress fiber. Bars, 10 µm and 3 µm in the main image and magnified panels, respectively. **(E)** Co-localization of myosin-18B-GFP with Tpm1.6-mCherry and F-actin in a U2OS cell. The insets demonstrate (1) the co-localization of myosin-18B and Tpm1.6 in ventral stress fibers, and (2) the lack of clear co-localization of perinuclear myosin-18B puncta with F-actin. Bars, 10 µm and 1 µm in the left and right magnified panels, respectively.

Figure S2

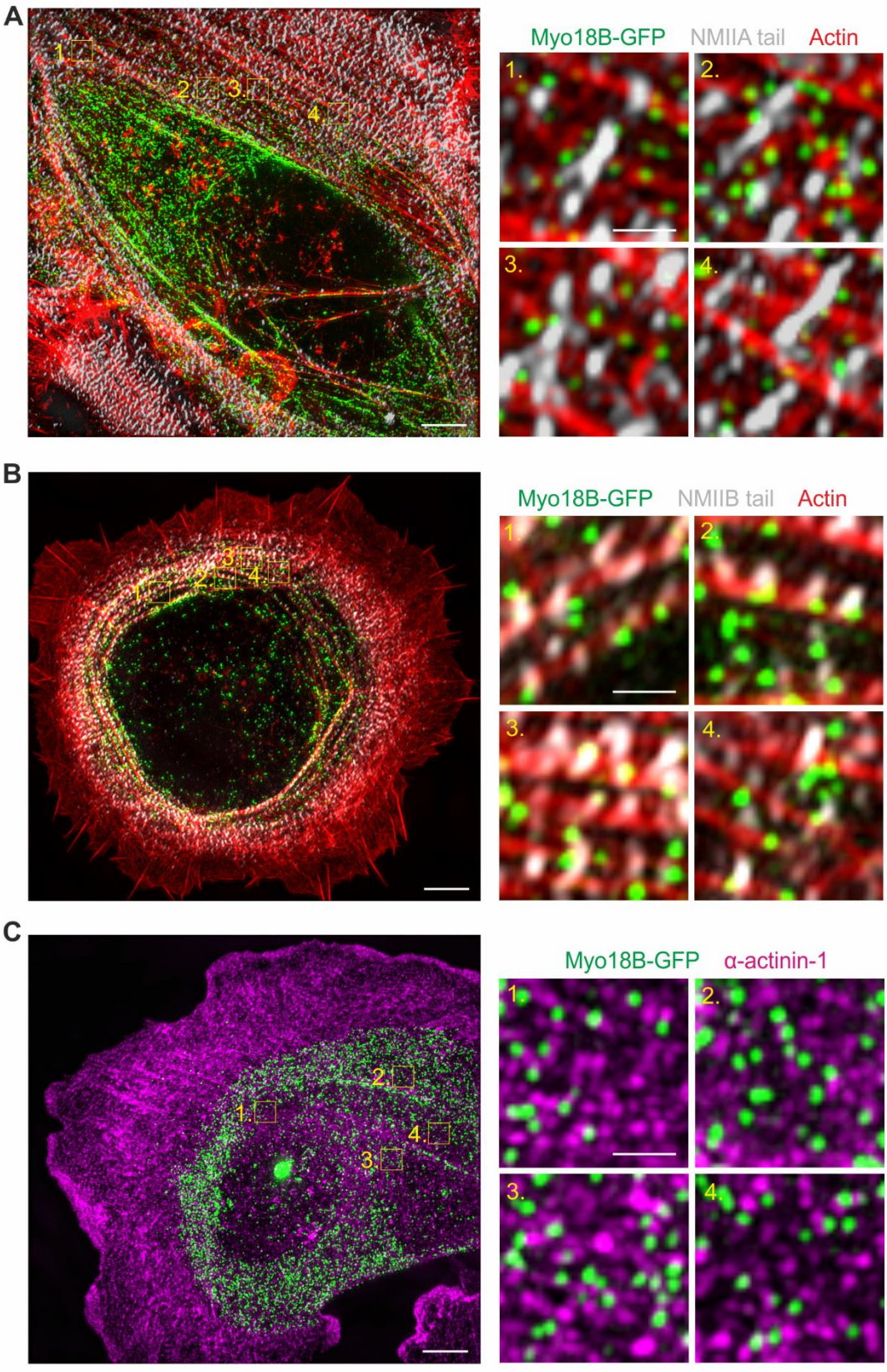
A
1.
2.
3.
4.
Myo18B-GFP
NMIIA tail
Actin
1.
2.
3.
4.
B
1.
2.
3.
4.
Myo18B-GFP
NMIIB tail
Actin
1.
2.
3.
4.
C
1.
2.
3.
4.
Myo18B-GFP
α-actinin-1
1.
2.
3.
4.

Figure S2 Myosin-18B localization by 3D-SIM. Related to Figure 2. (**A** and **B**) Representative examples of cells expressing myosin-18B-GFP. NMIIA tail (panel **A**), NMIIB tail (panel **B**), and actin were visualized by antibodies against NMIIA/B C-termini and phalloidin, respectively. Magnified regions illustrate different localization patterns observed for myosin-18B. (**C**) Representative example of a cell expressing myosin-18B-GFP and stained with an α-actinin-1 antibody. Magnified regions illustrate that myosin-18B does not display marked co-localization with α-actinin-1. Bars, 5 μm and 0.5 μm in the left and right magnified panels, respectively.

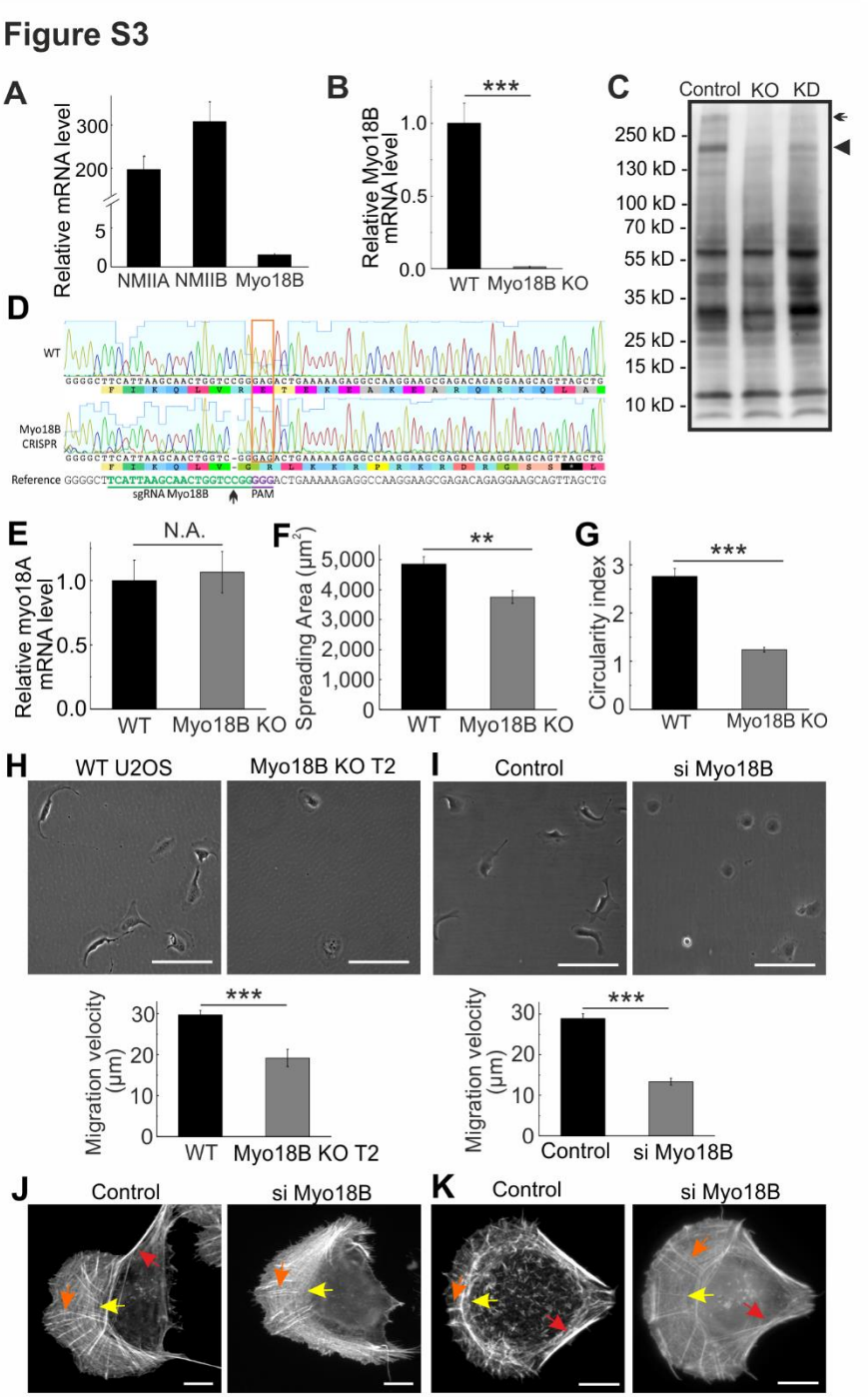

Figure S3 Myosin-18B knockdown and knockout phenotypes. Related to Figure 3. (**A**) Quantitative RT-PCR analysis demonstrating the relative transcript levels of NMIIA, NMIIB and myosin-18B. (**B**) Quantitative RT-PCR analysis demonstrating the loss of myosin-18B transcript in myosin-18B knockout cells. Quantifications are from three independent experiments. Data are represented as mean ± s.e.m. ***P = <0.001 (*t*-test). (**C**) Western blot analysis of endogenous myosin-18B levels in total cell lysates

of control, myosin-18B CRISPR/Cas9 knockout (KO) and myosin-18B siRNA knockdown (KD) U2OS cells. Please note that, in addition to the band of expected mobility (~280 kDa, arrow), also another band (corresponding to the mobility of ~200-230 kDa, arrowhead) is diminished in myosin-18B knockout cells compared to control cells. This probably corresponds to a lower molecular weight splice variant of myosin-1B, because according to the Uniprot database, there are two myosin-18B splice variants with molecular weights of ~285 kD and ~233 kD (accession No. Q8IUG5). (**D**) Sanger-sequencing analysis of the second exon targeted by sgRNA of the wild-type and myosin-18B knockout cell lines. Myosin-18B gene in the knockout cell line has a single nucleotide deletion in the 3rd position upstream of PAM sequence (arrow), resulting in a frame-shift, and consequent appearance of a stop codon 16 triplets downstream of a deletion point. Such premature termination in coding region produces 57 amino acids peptide, which most probably cannot carry out functions related to full length myosin-18B protein, which is 2 567 amino acids long. (**E**) Quantitative RT-PCR shows relative transcription levels of myosin-18A in wild-type and myosin-18B knockout cells. Quantifications are from three independent experiments. Data are represented as mean ± s.e.m. (**F**) Averaged spreading areas of wild-type and myosin-18B knockout cells. The data are presented as average cell size ± s.e.m, **P=<0.01 (*t*-test). n = 68 (for wild-type) and 32 (for myosin-18B knockout) cells. (**G**) Quantification of circularity index of wild-type and myosin-18B knockout U2OS cells shows that myosin-18B depletion results in cell rounding. The data are presented as average cell size ± s.e.m, ***P=<0.001 (t-test). n = 30 (for wild-type) and 30 (for myosin-18B knockout) cells. Circularity index = perimeter^2/(4π × area). (**H**) Representative images form time-lapse videos of wild-type, myosin-18B knockout exon 1 targeted (T2) cells migrating on a fibronectin-coated surface, and the corresponding random migration velocities. ***P = <0.001 (*t*-test). n= 36 for wild-type, and 29 for myosin-18B knockout (T2) cells. Bars, 50 µm. (**I**) Representative images form time-lapse videos of control and myosin-18B siRNA knockdown U2OS cells migrating on a fibronectin-coated surface, and the corresponding random migration velocities. ***P = <0.001 (*t*-test). n= 28 for control, and 26 for siRNA myosin-18B knockdown cells. Bars, 50 µm. The data are presented as average velocity obtained from a 12 hour cell tracking ± s.e.m. (**J and K**) Representative images of actin filaments visualized by phalloidin in control and myosin-18B siRNA knockdown U2OS cells plated on cover slips (J) and crossbow shaped micro-patterns (K). Bars, 10 µm.

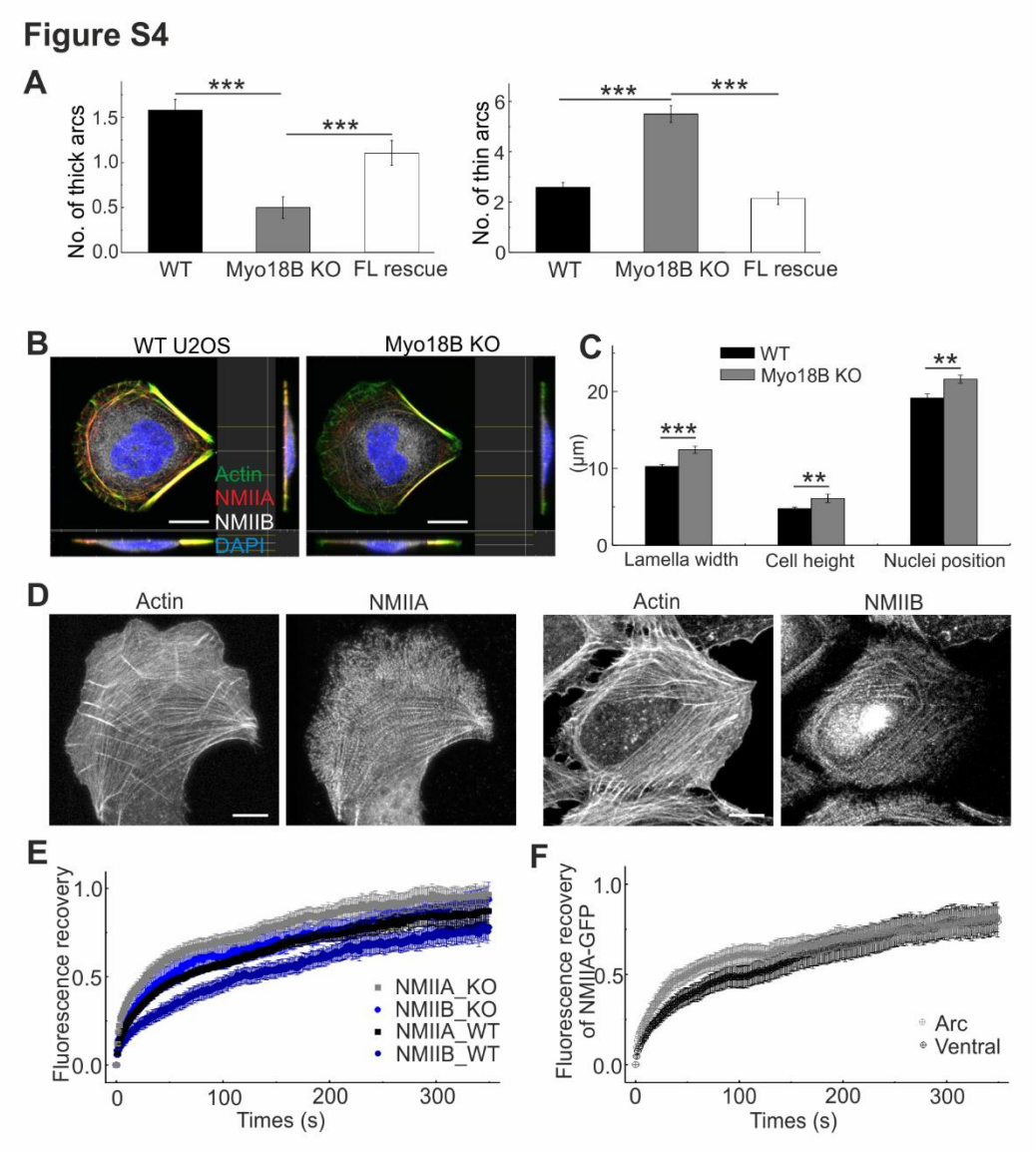

Figure S4 Myosin-18B knockout phenotypes. Related to Figure 4. (**A**) Blind manual quantification of the average numbers of thick and thin arcs in wild-type, myosin-18B knockout and full-length myosin-18B rescue (FL rescue) knockout cells plated in micro-patterns. See Fig. 3G for definition of thin and thick arcs. The data are presented as mean ± s.e.m. ***P=<0.001 (*t*-test). n = 32 for wild-type, 30 for myosin-18B knockout cells and 32 for rescue cells. (**B**) Representative cross sections of wild-type and myosin-18B knockout cells plated on crossbow shaped micro-patterns. Cells were visualized for F-actin, NMIIA and NMIIB. DAPI was used for nuclei staining. Bars, 10 µm. (**C**) Quantification of averaged lamella widths, cell heights, and distances of nuclei from the leading edge from wild-type and myosin-18B knockout cells plated on crossbow shaped micro-patterns. The data are presented as mean ± s.e.m. **P=<0.01, ***P=<0.001 (*t*-test). n = 13 for wild-type and 13 for myosin-18B knockout cells. (**D**)

NMIIA and NMIIB localize to thin arcs in myosin-18B knockout cells. Bars, 10 μm. (**E**) Normalized average FRAP recovery curves of NMIIA and NMIIB in stress fibers of wild-type (black and dark blue line) and myosin-18B knockout (grey and blue line) cells. 21 (wild-type) and 22 (knockout) GFP- NMIIA transfected cells, and 16 (wild-type) and 15 (knockout) GFP-NMIIB transfected cells were used for quantification. The data are presented as mean ± s.e.m. (**F**) Normalized average FRAP recovery curves of NMIIA in arcs (grey line) and ventral stress fibers (black line) of wild-type U2OS cells. The NMIIA recovery was quantified from 18 cells (for its dynamics in arcs) and 15 (for its dynamics in ventral stress fibers). The data are presented as mean ± s.e.m.

Figure S5

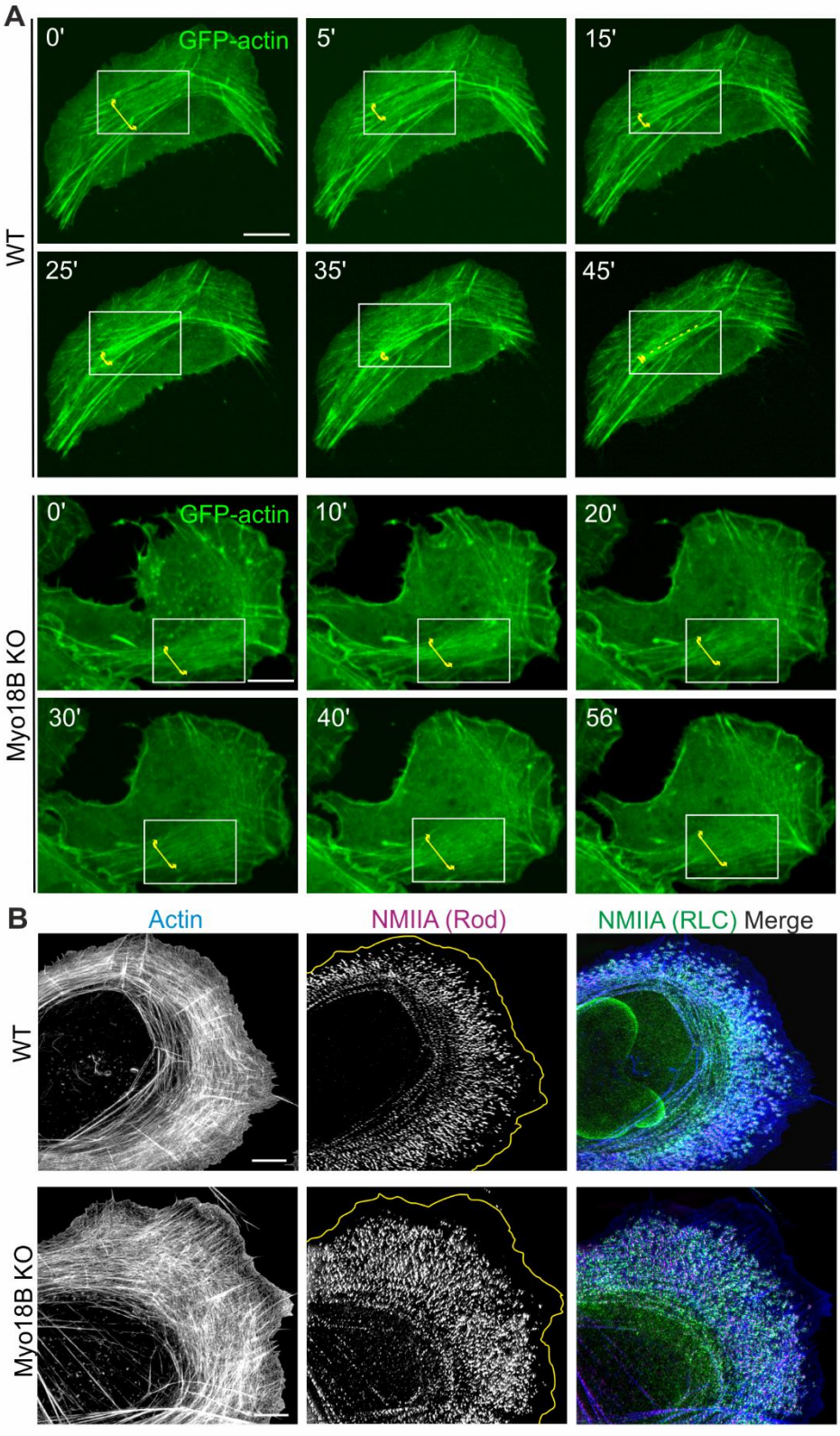
A
WT
0'
GFP-actin
5'
15'
25'
35'
45'
Myo18B KO
0'
GFP-actin
10'
20'
30'
40'
56'
B
Actin
NMIIA (Rod)
NMIIA (RLC) Merge
WT
Myo18B KO

Figure S5 Myosin-18B knockout cells display defects in maturation of ventral stress fibers from transverse arcs, and in the formation of NMII stacks. Related to Figures 4 and 5. (**A**) Representative time-lapse images of wild-type and myosin-18B knockout cells demonstrating the centripetal flow and fusion of transverse arcs. Yellow brackets highlight the fusion of transverse arcs into a ventral stress fiber in the wild-type, and centripetal flow of arcs without fusion in the myosin-18B knockout cell. Bars, 20 μm. (**B**) Representative 3D-SIM images of wild-type and myosin-18B knockout cells where actin, NMIIA motor and NMIIA tail domains were visualized by phalloidin, antibodies against regulatory light chain (RLC) and NMIIA C-terminus, respectively. Bars, 5 μm.

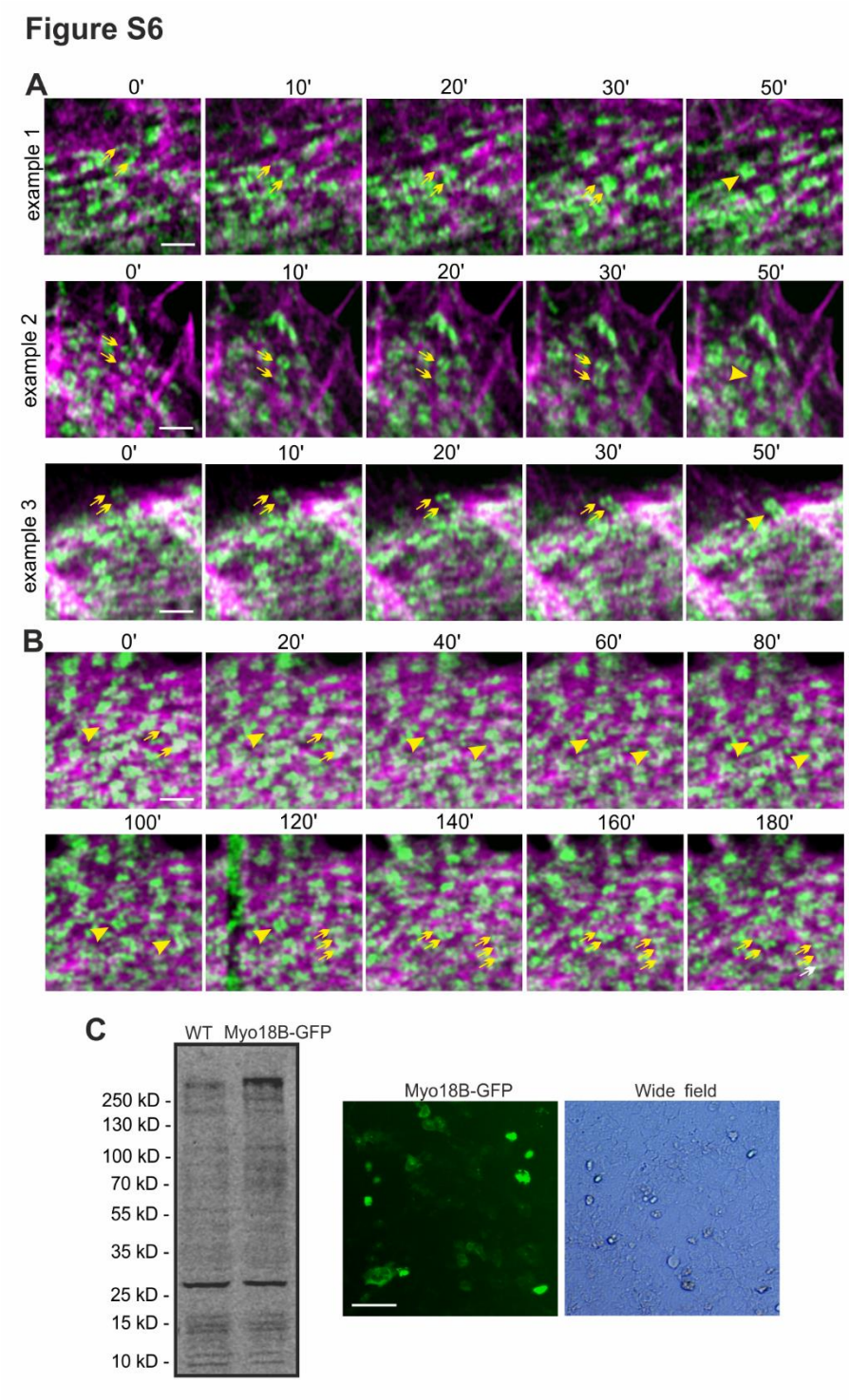

Figure S6 Zeiss Airyscan imaging of NMII stack fusion and splitting in wild-type and myosin-18B knockout cells, and the analysis of expression levels of myosin-18B in U2OS cells. Related to Figures 6 and 7. Representative time-lapse images of wild-type (**A**) and myosin-18B knockout U2OS (**B**), where NMIIA motor domain and actin were visualized by GFP-NMIIA and actin-RFP, respectively.

Three examples of myosin II filament fusion events (from two arrows to an arrowhead) are shown in panel (**A**), and two examples of myosin II stack splitting (from an arrowhead to arrows) are highlighted in panel (**B**). Bars, 1 μm. (**C**) Western blot analysis of myosin-18B levels in wild-type cells and in cells transiently transfected with a plasmid expressing myosin-18B-GFP (left). Fluorescence and wide-field imaging of the cells from the same experiments demonstrating the transfection efficiency. Only the cells with intermediate GFP intensity were used for further experiments. Based on this analysis, they expressed approximately 10-fold higher levels of myosin-18B-GFP compared to the levels of endogenous myosin-18B in U2OS cells. Bar, 100 μm.

Figure S7

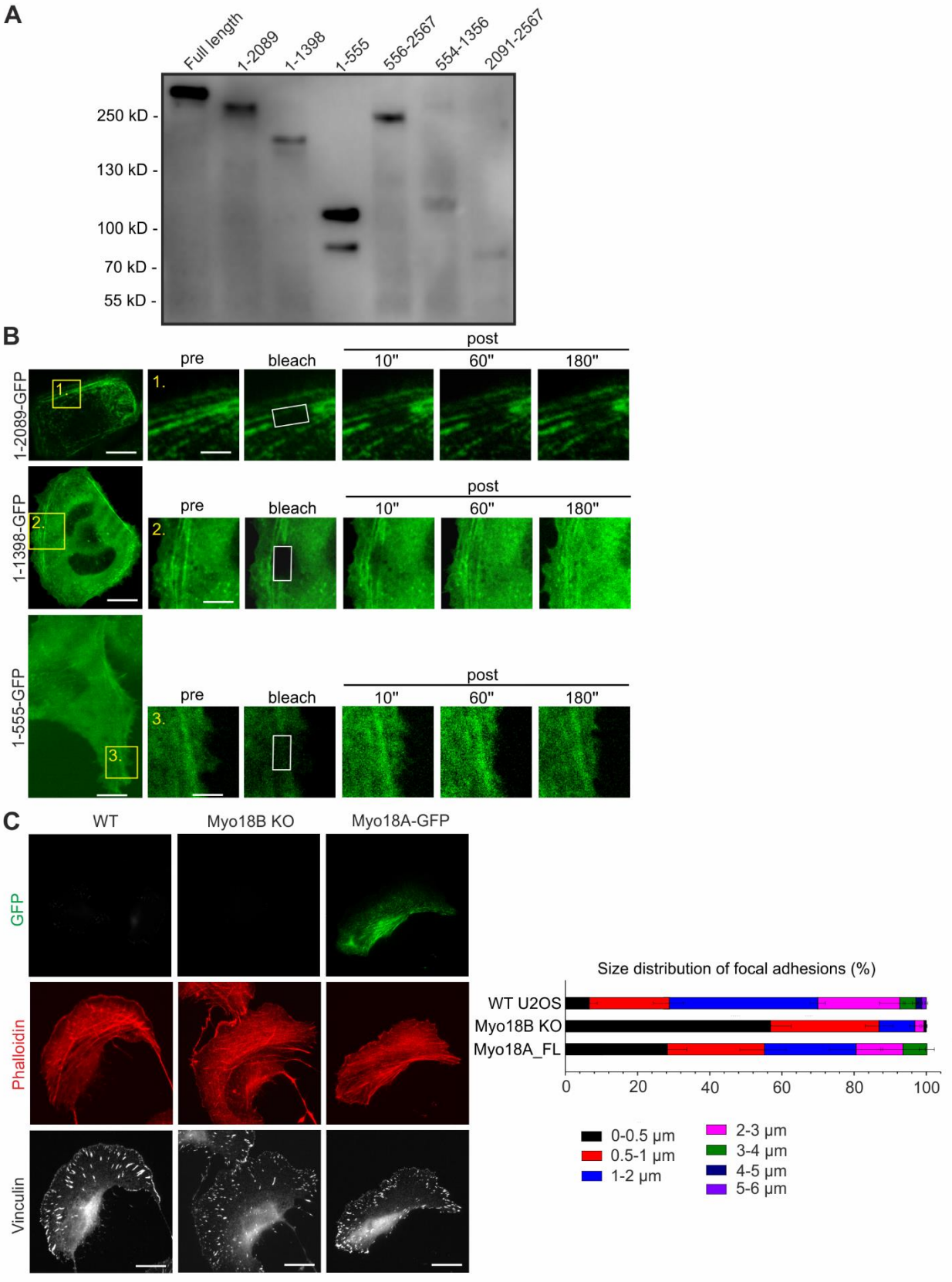
A
Full length
1-2089
1-1398
1-555
556-2567
554-1356
2091-2567
250 kD -
130 kD -
100 kD -
70 kD -
55 kD -
B
pre
bleach
post
10"
60"
180"
1-2089-GFP
1-1398-GFP
1-555-GFP
1.
2.
3.
C
WT
Myo18B KO
Myo18A-GFP
GFP
Phalloidin
Vinculin
Size distribution of focal adhesions (%)
WT U2OS
Myo18B KO
Myo18A_FL
0
20
40
60
80
100
0-0.5 µm
0.5-1 µm
1-2 µm
2-3 µm
3-4 µm
4-5 µm
5-6 µm

Figure S7 Dynamics of myosin-18B deletion constructs, and the rescue of myosin-18B knockout phenotype by over-expression of myosin-18A. Related to Figure 7. (**A**) The expression of myosin-18B-GFP constructs as detected by Western blot using GFP antibody. Please note that construct 1-555 showed two separate bands on Western blot. Thus, a fraction of the protein appears to be degraded when expressed in U2OS cells, and the mobility of 'un-degraded' fragment is slower than expected from its molecular weight. (**B**) Representative examples of the dynamics of different myosin18B-GFP constructs in myosin-18B knockout U2OS cells as examined by FRAP. Bars, 10 μm (in cell images) and 2 μm (in the magnified time-lapse images). Please note that only those Myosin-18B deletion constructs, which localized to stress fibers, were included in the FRAP analysis. **(C)** Left panel shows the representative images of wild-type cells, myosin-18B knockout cells, and myosin-18B knockout cells expressing a myosin-18A-GFP construct. F-actin and focal adhesions were visualized by fluorescent phalloidin and an antibody against vinculin, respectively. Bars, 10 μm. Right panel shows the length distributions of vinculin-positive focal adhesions. The number of focal adhesions in each size group was divided with the total adhesion number of the same cell. n = 652 adhesions from 10 cells (wild-type); 1864 adhesions from 12 cells (myosin-18B knockout,); 1436 adhesions from 16 cells (myosin-18A-GFP). Data are represented as mean ± s.e.m.

Table S1. Spectral count values of biotinylated proteins by BirA-tagged human tropomyosin-1.6 in U2OS cells. The data are from two independent experiments. Related to Figure 1.

Uniprot Accession	Protein Description	Spectral Count Value (Median)	Standard Error of Mean
Q8WZ42	Titin [TITIN_HUMAN]	528	10.59
Q15149	Plectin [PLEC_HUMAN]	280	6.49
P35579	Myosin-9 [MYH9_HUMAN]	259	12.05
P63261	Actin, cytoplasmic 2 [ACTG_HUMAN]	232.5	13.15
P09493	Tropomyosin alpha-1 chain [TPM1_HUMAN]	143.5	3.94
Q01082	Spectrin beta chain, non-erythrocytic 1 [SPTB2_HUMAN]	102	5.75
P68133	Actin, alpha skeletal muscle [ACTS_HUMAN]	99.5	3.03
Q05682	Caldesmon [CALD1_HUMAN]	95.5	2.93
P06753	Tropomyosin alpha-3 chain [TPM3_HUMAN]	94.5	2.48
P07951	Tropomyosin beta chain [TPM2_HUMAN]	92	2.25
P35749	Myosin-11 [MYH11_HUMAN]	87.5	5.55
Q13813	Spectrin alpha chain, non-erythrocytic 1 [SPTN1_HUMAN]	85.5	4.49
A5A3E0	POTE ankyrin domain family member F [POTEF_HUMAN]	80	4.41
P35580	Myosin-10 [MYH10_HUMAN]	79	4.41
P49454	Centromere protein F [CENPF_HUMAN]	78	4.09
Q9UHB6	LIM domain and actin-binding protein 1 [LIMA1_HUMAN]	77.5	6.82
Q14204	Cytoplasmic dynein 1 heavy chain 1 [DYHC1_HUMAN]	68.5	1.96
P0CG39	POTE ankyrin domain family member J[POTEJ_HUMAN]	66.5	4.53
Q562R1	Beta-actin-like protein 2 [ACTBL_HUMAN]	66	0.63
P15924	Desmoplakin [DESP_HUMAN]	65	3.35
O75165	DnaJ homolog subfamily C member 13 [DJC13_HUMAN]	63.5	2.69
Q8IZT6	Abnormal spindle-like microcephaly-associated protein [ASPM_HUMAN]	62.5	2.17
P46939	Utrophin [UTRO_HUMAN]	60.5	5.46
Q7Z7A1	Centriolin [CNTRL_HUMAN]	59.5	7.30
Q8IUG5	Unconventional myosin-XVIIIb[MY18B_HUMAN]	59.5	3.59
Q86V48	Leucine zipper protein 1[LUZP1_HUMAN]	59	4.13
P33176	Kinesin-1 heavy chain [KINH_HUMAN]	56	3.38
P67936	Tropomyosin alpha-4 chain [TPM4_HUMAN]	56	0.75
Q9P2D7	Dynein heavy chain 1, axonemal [DYH1_HUMAN]	55.5	6.36
Q5THJ4	Vacuolar protein sorting-associated protein 13D[VP13D_HUMAN]	53	1.66
Q15075	Early endosome antigen 1 [EEA1_HUMAN]	51.5	5.44
Q6UB98	Ankyrin repeat domain-containing protein 12 [ANR12_HUMAN]	50	2.87
Q16181	Septin-7 [SEPT7_HUMAN]	48.5	1.66
O75116	Rho-associated protein kinase 2 [ROCK2_HUMAN]	48	4.03
Q00610	Clathrin heavy chain 1 [CLH1_HUMAN]	47.5	0.71
P19338	Nucleolin [NUCL_HUMAN]	46	3.09
Q9UHD8	Septin-9 [SEPT9_HUMAN]	45.5	2.17
Q13315	Serine-protein kinase ATM [ATM_HUMAN]	45	3.34
Q9ULV4	Coronin-1C [COR1C_HUMAN]	45	0.82
P26038	Moesin [MOES_HUMAN]	43.5	2.25
Q15652	Probable JmjC domain-containing histone demethylation protein 2C [JHD2C_HUMAN]	43.5	3.14
Q9UPA5	Protein bassoon [BSN_HUMAN]	41	3.54
Q9Y6J0	Calcineurin-binding protein cabin-1 [CABIN_HUMAN]	40.5	3.86
O75534	Cold shock domain-containing protein E1 [CSDE1_HUMAN]	39	1.11
Q5VUA4	Zinc finger protein 318 [ZN318_HUMAN]	39	3.61
Q9BQE3	Tubulin alpha-1C chain [TBA1C_HUMAN]	38	0.75
Q9NVA2	Septin-11[SEP11_HUMAN]	38	2.06
O00159	Unconventional myosin-Ic [MYO1C_HUMAN]	37.5	3.97
Q5T5P2	Sickle tail protein homolog[SKT_HUMAN]	37.5	1.93
Q5T9S5	Coiled-coil domain-containing protein 18 [CCD18_HUMAN]	37	2.95

Table S2. Oligonucleotides used in this study. Related to STAR Methods.

Oligonucleotides	
siRNA pool of myosin-18B	5' GCAGAAAGGCCUCGGAUAC 3', 5' AAUCAGAGAAGUUGCGGAA 3', 5' GAGAACAUGACGCGGAACA 3', 5' CGGCAAAAGTACUGTCAUU 3'
siRNA pool of myosin-18A	5' CCAAGAAACACGGGCGUAA 3', 5' AGGAAGACAUGAACGAAUU 3', 5' CAAUGGAGGUGGAGAUCGA 3', 5' UGAAAGGACGCAAGUGAA 3'
Myosin-18B CRISPR constructs T1	Forward: 5' CACCGCTCATCACGCCTCGCCCTGT 3' Reverse: 5' AAACACAGGGCGAGGCGTGATGAGC 3'
Myosin-18B CRISPR constructs T2	Forward: 5' CACCGTCATTAAGCAACTGGTCCGG 3' Reverse: 5' AAACCCGGACCAGTTGCTTAATGAC 3'
Oligoes for sequencing to confirm the myosin-18B CRISPR knockout	5' ATCTCATGTGCTGCGTGTGTC 3' 5' CTCGCTCTCCTTGCCCAGAAT 3' 5' GCCTCTTTCAGCTCTGTGGTC 3'
Oligoes for sanger-sequence	5' ATTCGGGAAGAGGACAAGAGC 3'
Oligoes for Illumina next generation sequencing	5' CTTGGTCATGTATGTCTCCTC 3' 5' GGATGACAAATGACTCAGAGG 3'
Oligoes for cloning mCherry-myosin-18B-GFP	5' GACTCAGATCTCGAGCTATGGCCATCTCATCACGCCTCGCC 3' 5' TATGGCTGATTATGATCAGTTATCTACTTGTACAGCTCGTCCATGCCGAGAGTG 3'
Oligoes for cloning myosin-18B-GFP (1-1398)	5' CGGACTCAGATCTATGGCCATCTCATCACGCCTCGCC 3' 5' ATTATGATCAGTTAGGTGGCACTAAGTAGAGGCTGGAGGGAAC 3'
Oligoes for cloning myosin-18B-GFP (2091-2567)	5' CGGACTCAGATCTCCTCTACTTAGTGCCACCATTGGAACTG 3' 5' ATTATGATCAGTTACTTCTGGAGGTATTTCTTCATTATGCTCGCAAC 3'
Oligoes for myosin-18B in RT-PCR	Forward: 5' ATGGCCATCTCATCACGCCTC 3' Reverse: 5' GCCTCTTTCAGCTCTGTGGTC 3'
Oligoes for myosin-18A in RT-PCR	Forward: 5' GGACATGGTGACAAAGTATCAGAA 3' Reverse: 5' TTTGACAACCAGGACTTGACC 3'